SUPPLEMENTAL INFORMATION

METHODS

Animals. Adult (9-11 week-old) male mice were housed 3 per cage under controlled illumination (12:12 h light/dark cycle; light on 06.00 AM) and environmental conditions (room temperature 20 – 22 °C, humidity 55–60%) for at least 1 week before experiments. Mouse chow and tap water were available *ad libitum*. The experimental procedures were approved by the Animal Ethics Committee of the Second University of Naples. Animal care was in compliance with the IASP and European Community (E.C. L358/1 18/12/86) guidelines on the use and protection of animals in experimental research. All efforts were made to minimize animal suffering and to reduce the number of animals used. For the purposes of our study we employed the following types of animals:

a) Adult male leptin knockout *ob/ob* mice (JAK® mice strain) B6.V-Lep^{ob}/J matched to wt littermates leptin gene expressing homozygous siblings feed ad libitum through a standard laboratory regimen (3.5 kcal/g, 14.5% of energy as fat).

b) High fat diet-induced obese C57BL/6J male mice (HFD, 16-18 week old), made obese after 7 weeks of high fat diet (4.7 kcal/g: 49% fat, 18% protein and 33% carbohydrate) matched to lean male mice 16-18 week old feed with standard fat diet (SFD) (3.5 kcal/g, 14.5% of energy as fat; **Figure S*1A*** for details). Serum leptin (Quantikine M; R&D Systems) levels were determined using commercial sandwich ELISA assays (B-Bridge International) in accordance with the manufacturer's instructions.

Intra-VL PAG microinjections

Direct intra-vlPAG administration of drugs, or respective vehicle, was conducted with a stainless steel cannula connected by a polyethylene tube to a SGE 1-microlitre syringe, inserted through the guide cannula and extended 1 mm beyond the tip of the guide cannula to reach the vlPAG. Vehicle or drug solutions were administered into the vlPAG in a final volume of 0.8 uL. Microinjection was performed over a period of 60 sec and the injection cannula gently removed 2 min later. At the end of the experiment, a volume of 0.8 µL of neutral red (0.1%) was also injected into the vlPAG 30-40 min before killing the mouse. Mice were then perfused intracardially with 20 ml phosphate buffer solution (PBS) followed by 200 ml 10% formalin solution in PBS. The brains were removed and immersed in a saturated formalin solution for 2 days. The injection sites were ascertained by using 2 consecutive sections (40 µm), one stained with cresyl violet to identify

nuclei and the other unstained in order to determine dye spreading. Only the mice whose microinjected site was located within the vlPAG were used for data computation.

RVM in vivo extracellular recordings

We used a David Kopf stereotaxic apparatus (David Kopf Instruments, Tujunga, CA, USA) with the animal positioned on a homeothermic temperature control blanket (Harvard Apparatus Limited, Edenbridge, Kent). After implantation of the guide cannula into the vlPAG, a glass insulated tungsten filament electrode (3-5 MΩ) (Frederick Haer & Co., ME, USA) was stereotaxically lowered, through a small craniotomy, into the RVM (6,48 mm caudal to bregma, 0.3-0.5 mm lateral and 4,5-6 mm depth from the surface of the brain) using the coordinates from the atlas of Paxinos and Watson (1986). The jugular vein was cannulated to allow intravenous anaesthetic administration (propofol, 8-10 mg/kg/h, i.v.). The RVM ON cells were identified by a burst of activity that begins just after mechanical stimulus applied on the hind paw while OFF cells were identified by the fact that they cease firing at that time. Mechanical stimuli were applied using a spring-operated forceps with a force (>300g/10 mm^2 and < 400 g/10 mm^2) that squeezed the tissue (painful pressure). Nociceptive stimuli were elicited every 5 min for at least 15 min prior to microinjecting drugs, or the respective vehicle, artificial cerebrospinal fluid (composition in mM: KCl 2.5; NaCl 125; $MgCl_2$ 1.18; $CaCl_2$ 1.26) into the vlPAG. The recorded signals were amplified and displayed on (an) analog and digital storage oscilloscope to ensure that the unit under study was unambiguously discriminated throughout the experiment. Signals were also processed by an interface (CED 1401) (Cambridge Electronic Design Ltd., UK) connected to a Pentium III PC. Spike2 software (CED, version 4) was used to create peristimulus rate histograms on-line and to store and analyse digital records of single-unit activity off-line. Configuration, shape, and height of the recorded action potentials were monitored and recorded continuously, using a window discriminator and Spike2 software for on-line and off-line analysis. Once an RVM cell was identified from its background activity, we optimised spike size before all treatments. This study only included neurons whose spike configuration remained constant and could clearly be discriminated from activity in the background throughout the experiment, indicating that the activity from one neuron only and from the same one neuron was measured. After fixation by immersion in a 10% formalin, the recording sites were identified. In each mouse, only one neuron was recorded before and after vehicle or drug administration. The neuron responses, before and after intra-vlPAG vehicle or drug microinjections were measured and expressed as spikes/sec (Hz). At the end of the experiment, each animal was killed with a lethal dose of urethane, the microinjection site was marked with 0.2 μl of a Cresyl Violet solution and the recording site marked

with a 20 µA DC current for 20 s. After fixation by immersion in 10% formalin, the microinjection and recording sites were identified.

Patch Clamp recordings

In order to test for the respective intrinsic membrane properties, the neuron‘s membrane potential was held at about -60 mV in current clamp. Neurons were regarded as being GABAergic interneurons when depolarizing current pulses caused high frequent, non-adapting spiking (frequency ≥ 20Hz), and when hyperpolarizing current pulses caused the neuron to fire an action potential (a low-threshold spike, LTS) during the re-polarization of the membrane). Since vlPAG neurons projecting to the RVM (vlPAG-RVM neurons) do not display LTS when tested with hyperpolarizing current pulses, they are currently separated into two populations, namely, fast spiking (FS) and transient spiking (TS) neurons. FS vlPAG-RVM neurons display high frequent spiking (≥ 20Hz), with an initial adaptation in spiking, and TS vlPAG-RVM neurons exhibit low frequency spiking (< 20Hz). To confirm the validity of these criteria, we injected the retrograde tracer Cholera Toxin subunit B carrying Alexa Fluor® 488 (CT-B) (Life Technologies, Carlsbad, CA, USA) into the RVM (coordinates: 6,48 mm caudal to bregma, 0.3-0.5 mm lateral and 4,5-6 mm depth from the surface of the brain). 10 - 12 days after the injection the mice were anesthetized and coronal midbrain slices were prepared, as described above. CT-B labeled neurons were visualized using a Leica DM6000 FS microscope (Leica Microsystems, Wetzlar Germany) equipped with an appropriate filter and a camera (WAT-902H Ultimate, Watec Co. Ltd., Tsuruoka-Shi, Yamagata-Ken, Japan). Once visually identified, the intrinsic membrane properties of four CT-B labeled wt vlPAG neurons were examined and were found to exhibit the same membrane properties as described elsewhere (**Park et al., 2010**) Hence, recordings obtained from these neurons were pooled together with those obtained from not-labeled neurons.

Immunohistochemistry

All the animals were deeply anesthetized with a mixture of ketamine–xylazine (25 mg/ml ketamine, 5 mg/ml xylazine, 0.1% w/w pipolphen in H_2O; 1 ml/100 g, i.p.). Animals were then perfused transcardially with 0.9% saline for 5 min, followed by 100 ml of fixative containing 4% paraformaldehyde in 0.1 M phosphate buffer (PB), pH 7.4, for 20 min. The fixative of the mice for the electron microscopy studies contained 3% paraformaldehyde and 0.5% glutaraldehyde. The brains for double immunogold histochemistry were cut 50-µm-thick coronal sections by Leica VTS-1000 vibratome whereas the brains for immunofluorescence and peroxidase-based immunohistochemistry were cut with Leica CM3050S cryostate in serial coronal frozen sections (6-

10 μm-thick) collected onto electrostatic charged Menzel Super frost slides (Menzel Thermo Fisher Scientific, Germany) in three alternate series. For single based-immunoperoxidase procedure, the sections were incubated with specific normal serum-diluted primary polyclonal antibody goat anti-OX-A (Santa Cruz Biotechnology) revealed by specific biotinylated secondary anti-IgGs (Vector Laboratories, Burlingame, CA) followed by incubation in the avidin-biotin complex (ABC Kit; Vectastain, Vector) and 3-3' diaminobenzidine revelation (DAB Sigma Fast, Sigma-Aldrich, Louis, MO U.S.A.). Quantitative analysis of the intensity of OX-A immunostaining was performed by using digital camera working on grey levels (JCV FC 340FX, Leica) for image acquisition and by using the image analysis software Image Pro Plus® 6.0 (MediaCybernetics) working on a logarithmic scale of absorbance, for the densitometric evaluation of OX-A expression in fibers projecting to vlPAG. This latter was performed by applying an imaginary box surrounding the entire vlPAG identified according the Paxinoxs's Atlas of the mouse brain (n=20 sections per mouse). The images for densitometric analysis were acquired under constant light illumination and magnification. In each section the zero value of optical density was assigned to the portion of tissue devoid of OX-A immunoreactivity. For multiple immunofluorescence the sections were incubated in a mixture of anti-OX-A/synaptophysin or CB_1/synaptophysin or OX-1R/DAGLα primary antibodies (all diluted 1:100-1:300 in donkey serum). Multiple immunofluorescence was revealed by specific mixture of Alexa546/Alexa350 secondary donkey anti-IgGs. Controls of specificity for immunfluorescence labeling were performed by omission of each mixture of primary and/or secondary antibodies and by pre adsorbtion of each primary antibody with the respective blocking peptide. The sections processed for immunofluorescence were observed by confocal laser scanning microscope (LSM510 Meta, Zeiss), or fluorescence microscope equipped with the appropriate filters, equipped with deconvolution system (Leica DMI6000B). Images were acquired by digital camera Leica DFC420. Image analysis was performed by Leica MM AF analysis offline software working on Z-stack acquisition and deconvolution process (Leica, Germany). No labeling was detected in each control performed for reaction of multiple immunofluorescence

Preembedding immunogold labeling

CB_1/DAGLα or OX-1R/DAGLα or CB_1/OX-1R double pre-embedding immunogold labeling were performed on the vlPAG area of obese and lean mice according to the method described elsewhere **(Cristino et al., 2013**). At this purpose the sections were pretreated with PB containing 0.1% sodium borohydride for 1 min, washed PB three times for 15 min once and exposed to a blocking solution with 5% normal donkey serum and 0.1% saponin for 2 hour at room temperature and with gentle agitation. Sections were incubated with a blocking solution containing 0.02 %

saponin (in order to potentiate antibody penetration) and different mixture of primary antibodies as: 1) rabbit anti-CB_1 and guinea pig anti-DAGLα antibodies; 2) goat anti-OX-1R and guinea pig anti-DAGLα antibodies; 3) goat anti-OX-1R and rabbit anti-CB_1 revealed by mixture of 6 nm or 10 nm gold-conjugated secondary antibodies, diluted 1:30 in blocking solution containing saponin 0.02 %. In particular, appropriate 10nm gold-conjugated secondary antibodies were used to reveal DAGLα immunoreactivity vs 6nm gold-conjugated secondary antibodies for CB1 or OX-1R reactivities, whereas appropriate 6nm gold-conjugated secondary antibody revealed DAGLα immunreactivity *vs* 10nm gold-conjugated secondary antibodies for OX-1R reactivity. Negative controls were performed by omitting one or both of the primary or the secondary antibodies from the mixture. No labeling was detected in these controls of immunogold labeling. The sections were then treated with 0.5% OsO_4 in PB for 10 min at 4°C, dehydrated in an ascending series of ethanol and propylene oxide, and embedded in TAAB 812 resin (TAAB, England). During dehydration, sections were treated with 1% uranyl acetate in 70% ethanol for 15 min at 4°C. Ultrathin (60 nm) sections were collected on Formvar-coated single- or multiple-slot (50 mesh) grids and 0.65% lead citrate for 3 min. Electron micrographs were taken with the TEM microscope LEO 912AB (Zeiss, Germany).

Western blot

Mice were decapitated and brains were rapidly removed and frozen. The vlPAG were dissected on ice and homogenized in cold lysis buffer containing 10X TNE (50 mM Tris-HCl, pH 7.4, 150 mM NaCl, 10 mM EDTA), 10% Triton X-100, 100X Protease Inhibitor Cocktail (Sigma-Aldrich), 100X Phosphatase Inhibitor Cocktail 2 and 3 (Sigma-Aldrich). The lysates were centrifuged for 15 min at 15,000*g* at 4 °C and the supernatants were collected and stored at −20 °C until use. The concentration of protein was determined in duplicate the Lowry protein assay. Appropriate volumes of sample buffer and beta-mercaptoethanol were added to the homogenates, and samples were boiled for 10 min. Twenty micrograms of protein were electrophoresed on 10% polyacrylamide SDS–PAGE gels. Proteins were electro transferred onto PVDF membranes. The nonspecific binding of immunoproteins was blocked with 5% non-fat dry powdered milk dissolved in Tris-buffered saline (TBS) for 2 h at room temperature (RT). After blocking, the membranes were incubated with primary antibodies overnight at 4 °C. Primary antibodies phospho-STAT3 Tyr705 (1:1000, #4438G Invitrogen) and STAT3 (1:5000, #ab119352 Abcam) were dissolved in TBS containing 5% non-fat powdered milk. The membranes were rinsed three times for 10 min in TBS and three times for 10 min in TBS containing 0.1% Tween 20 (TBS-T), followed by 1 h incubation with HRP-conjugated anti-rabbit secondary antibody at RT. After incubation the

membranes were washed six times for 10 min in TBS-T and incubated with an enhanced chemiluminescence reagent (Clarity ECL, Biorad). The protein bands were visualized on ChemiDoc™ MP System (Biorad). The bands were quantified by Image J software, and standardized to β-actin (1:4000, #A1978, Sigma- Aldrich). With this software the optical density of the protein bands was measured. Results were expressed in ordinary unit density. The phosphorylation of the STAT 3 was evaluated by dividing the phospho-specific form by the no phosphorylated form of STAT3.

CB_1-β-arrestin2 co-immunoprecipitation

Mice were decapitated and brains were rapidly removed and frozen. vlPAG were dissected on ice and homogenized in ice cold lyses buffer containing 50 mM Tris–HCl, pH 7.5, 150 mM NaCl, 1 mM EDTA, 1 mM EGTA, 1% Triton and 10X Protease Inhibitor Cocktail (Sigma-Aldrich). The lysates were incubated on a rotating wheel for 30 min at 4 °C and then centrifuged at 13,000×g for 15 min at 4 °C to remove insoluble debris. Protein concentrations in the supernatants were determined in duplicate using the Lowry protein assay. The Co-Immunoprecipitation was performed by the Dynabeads Protein G-Kit (Invitrogen). All Invitrogen buffers were used according the manufacture's instruction. Briefly, the beads were incubated with 10 mg of anti-Cannabinoid Receptor CB1 Antibody (Calbiochem) for 30 min at room temperature (RT) under rotation. Following several washes the bound bead/antibody complex was added to 1.0 mg of sample protein for 45 min at RT under rotation. After washing, the captured bead/ProteinG/antigen complex was eluted with a Elution Buffer by heating at 70 °C for 10 min and the IPed proteins were analyzed by western blotting. 15 μg of IPed proteins were separated by SDS-polyacrylamide (10% gel) and transferred to a nitrocellulose membranes which were subsequently blocked with 5% nonfat powdered milk in TBS for 2h at RT. The membranes were incubated with the primary polyclonal antibodies anti-Cannabinoid receptor CB1 (1:500, Calbiochem) and anti-β-arrestin 2 (1:500, Cell Signalling), overnight at 4°C. Finally, the membranes were incubated with goat anti-rabbit IgG HRP (1:1500, Biorad) before ECL reagent (Biorad) and detection of signals to the ChemiDoc ™ (Biorad).

Lipid extraction and endocannabinoid measurement

Tissue samples from the LH were homogenized in 5 volumes of chloroform/methanol/Tris HCl 50 mM (2:1:1 by volume) containing 10 pmol of d^8-AEA and 50 pmol of d^5-2AG. Homogenates were centrifuged at 13,000 *g*/min for 16 min (4°C), the aqueous phase plus debris were collected and four times extracted with 1 vol of chloroform. The lipid-containing organic phases were dried down and pre-purified by open bed chromatography on silica columns eluted with increasing concentrations of methanol in chloroform. Fractions for AEA and 2-AG

measurements were obtained by eluting the columns with 9:1 (by vol.) chloroform/methanol and then directly analyzed by liquid chromatography-atmospheric pressure chemical ionization-mass spectrometry (LC-APCI-MS). LC-APCI-MS analyses were carried out in the selected ion monitoring (SIM) mode, using *m/z* values of 356 and 348 (molecular ions +1 for deuterated and undeuterated anandamide), 384.35 and 379.35 (molecular ions +1 for deuterated and undeuterated 2-AG)). AEA and 2-AG levels were therefore calculated on the basis of their area ratios with the internal deuterated standard signal areas, their amounts in pmols normalized per mg of lipids and compared by ANOVA followed by the Bonferroni's test.

Statistical analysis

The differences between lean (wt and SFD) and obese (*ob/ob* and HFD) mice were examined by applying the two-sample t-test. A p-value of less than 0.05 was considered statistically significant. Calculations were performed using SYSTAT (SPSS Inc., 1998; Version 9). For the patch-clamp electrophysiological studies the difference between vl-PAG untreated (control) neurons and neurons treated with SB were analyzed by employing the paired t-test. In case data were not normally distributed, differences between neurons of wt and *ob/ob* mice were analyzed with the Mann-Whitney U test. Generally, a p-value of less than 0.05 was considered statistically significant. Calculations were performed using SYSTAT (SPSS Inc., 1998; Version 9).

Figure S1

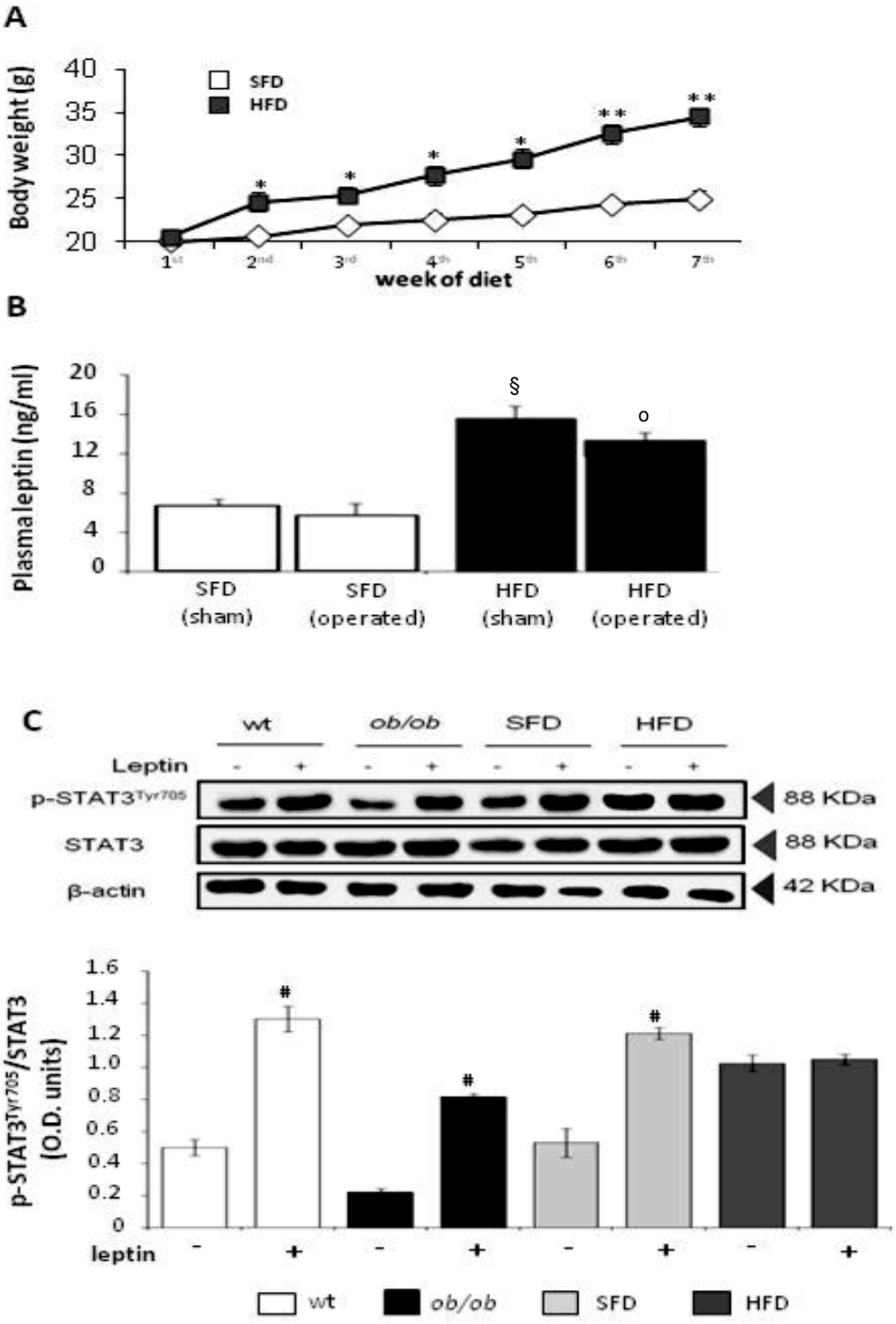
A
Body weight (g)
40
35
30
25
20
SFD
HFD
*
*
*
*
**
**
1st
2nd
3rd
4th
5th
6th
7th
week of diet
B
Plasma leptin (ng/ml)
20
16
12
8
4
0
§
o
SFD (sham)
SFD (operated)
HFD (sham)
HFD (operated)
C
wt
ob/ob
SFD
HFD
Leptin
- + - + - + - +
p-STAT3Tyr705
STAT3
β-actin
88 KDa
88 KDa
42 KDa
p-STAT3Tyr705/STAT3 (O.D. units)
1.6
1.4
1.2
1.0
0.8
0.6
0.4
0.2
0
#
#
#
leptin
- + - + - + - +
wt
ob/ob
SFD
HFD

FIGURE S1. Body weight, plasma leptin profile and central leptin sensitivity in lean and obese mice. (**A**) Time-course profile of the body weight of mice fed either with a standard fat diet (SFD) or with a high-fat diet (HFD) for 7 weeks, starting from the 9th week of age. *n* = 12 mice per group; means ± SEM; **P* < 0.05 (P=0.003; $F_{(1,14)}$=21.83); ** *P* < 0.01 (P=0.008; $F_{(1,18)}$=16.22) by comparison of HFD vs SFD. (**B**) Analysis of leptin plasma levels after the 7th week of sham or spared nerve injured (operated) SFD and HFD mice. **(C)** Representative western blot analysis of STAT3 phosphorylation on the Tyr705 residue as measure of the leptin receptor sensitivity in the vlPAG of obese (*ob/ob* and HFD) mice and matched lean (wt and SFD) control mice. Data are means ± SEM, n = 3 mice per group. § *P* < 0.005 by comparison of sham HFD to sham SFD; ^{o} *P* < 0.005 (P=0.002; $F_{(1,19)}$=12.03) by comparison of operated HFD to operated SFD; # *P* < 0.01 (P=0.009; $F_{(1,15)}$=20.12) by comparison of leptin-treated vs leptin-untreated mice. *P* values indicate statistically significant difference by two-way ANOVA followed by Bonferroni *post-hoc* test.

Figure S2

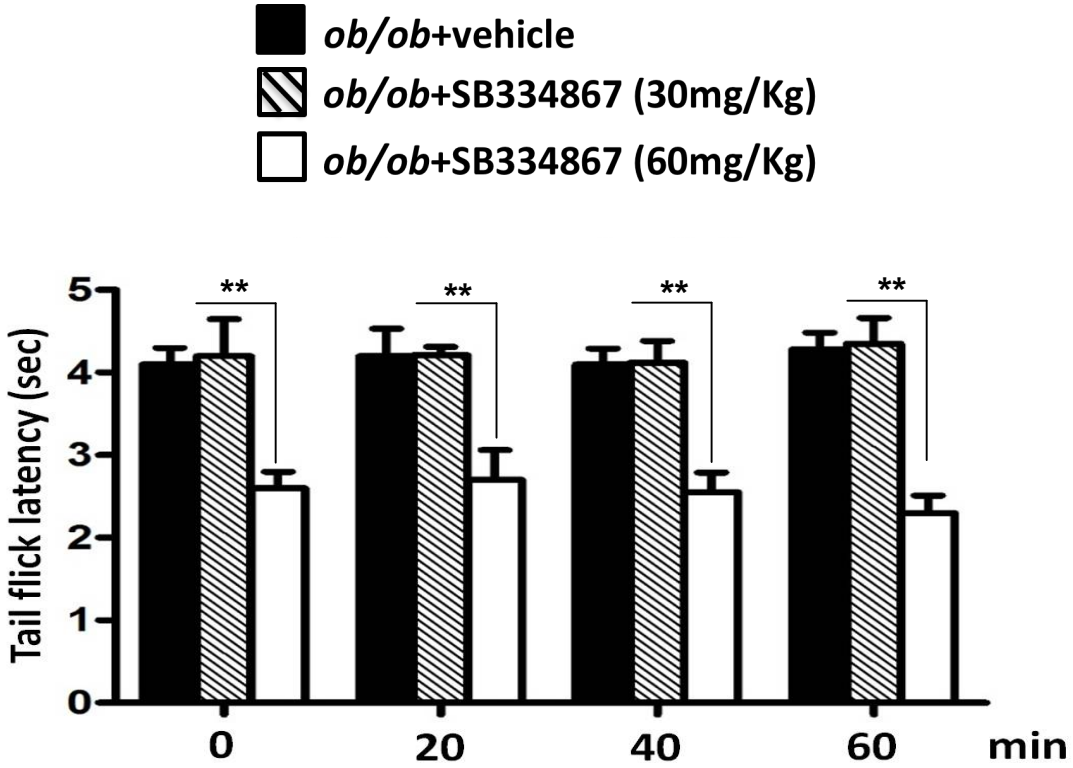

FIGURE S2. Identification of PAG output neurons to ON and OFF cells by CTB retrograde-tracing injection in RVM. (**A-C**) Arrows point to the same CTB-retrograde labeled cells receiving OX-A/synaptophysin-positive synapses (**A**) CB_1/synaptophysin-positive synapses (**B**) and coexpressing OX1-R and DAGLα in the somata (**C**). The area in the squares show the landmark region of adjacent sections (rectangular shape for A *vs* B, and square shape for B *vs C*).

Figure S3

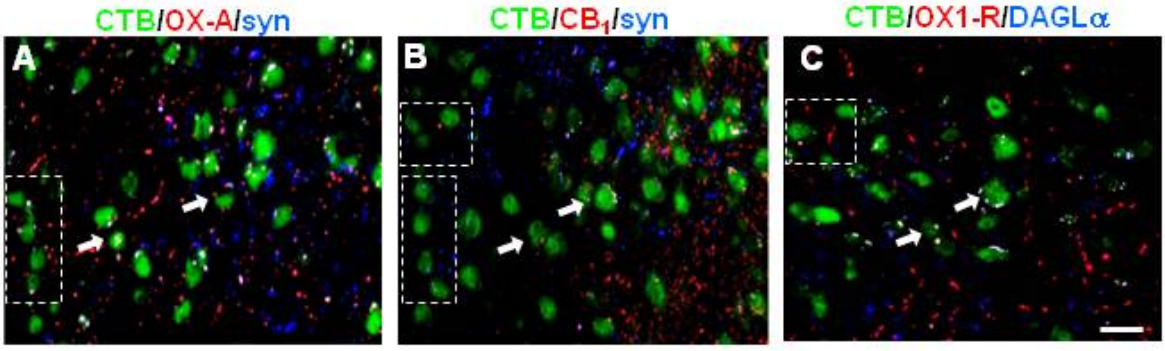

FIGURE S3. Identification of PAG output neurons to ON and OFF cells by CTB retrograde-tracing injection in RVM. (**A-C**) Arrows point to the same CTB-retrograde labeled cells receiving OX-A/synaptophysin-positive synapses (**A**) CB_1/synaptophysin-positive synapses (**B**) and coexpressing OX1-R and DAGLα in the somata (**C**). The area in the squares show the landmark region of adjacent sections (rectangular shape for A *vs* B, and square shape for B *vs C*).

Figure S4

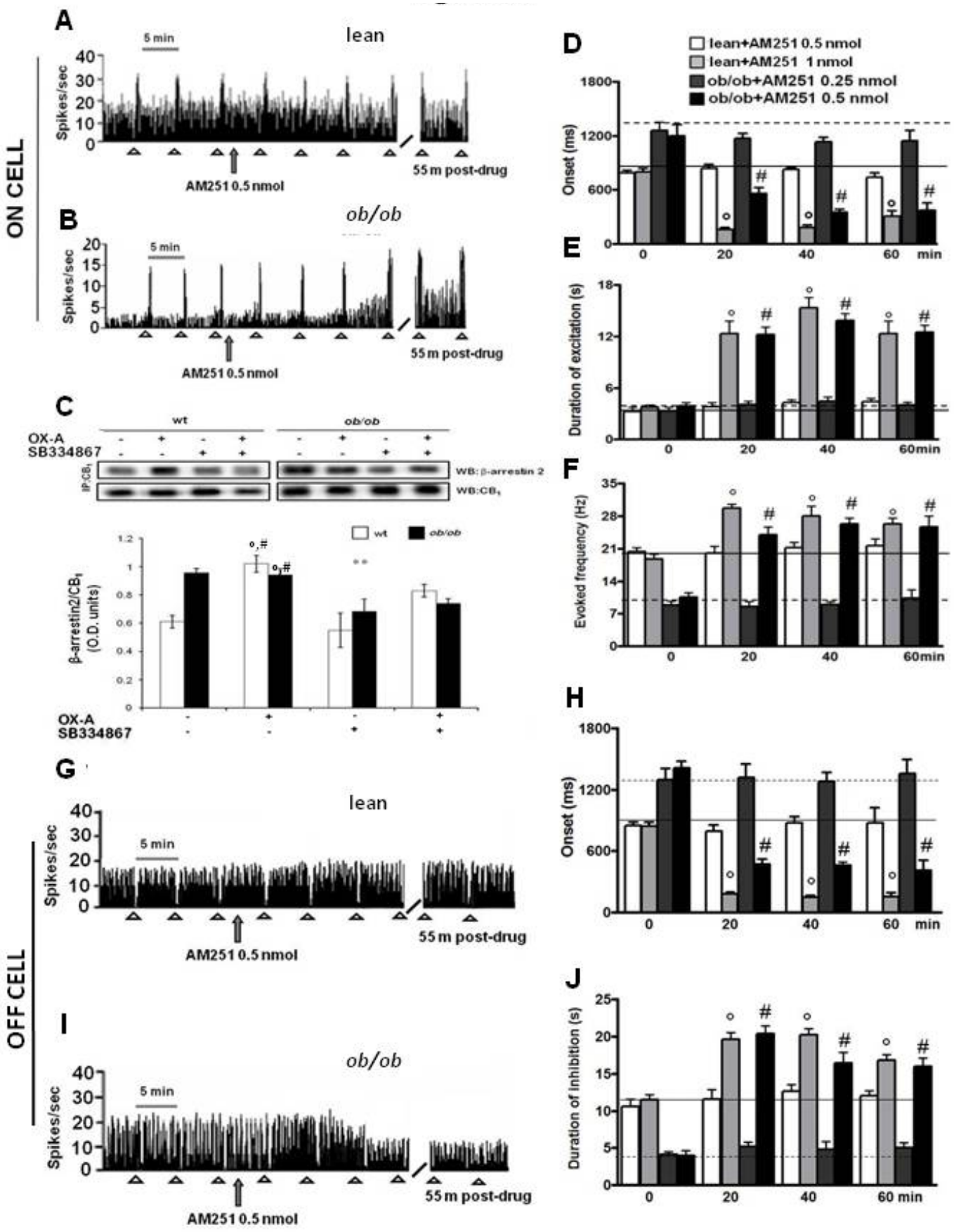
A
lean
5 min
Spikes/sec
AM251 0.5 nmol
55 m post-drug
ON CELL
B
ob/ob
5 min
Spikes/sec
AM251 0.5 nmol
55 m post-drug
C
wt
ob/ob
OX-A
SB334867
IP-CB1
WB: β-arrestin 2
WB:CB1
β-arrestin2/CB1 (O.D. units)
wt
ob/ob
OX-A
SB334867
D
lean+AM251 0.5 nmol
lean+AM251 1 nmol
ob/ob+AM251 0.25 nmol
ob/ob+AM251 0.5 nmol
Onset (ms)
E
Duration of excitation (s)
min
F
Evoked frequency (Hz)
60min
G
lean
5 min
Spikes/sec
AM251 0.5 nmol
55 m post-drug
OFF CELL
H
Onset (ms)
min
I
ob/ob
5 min
Spikes/sec
AM251 0.5 nmol
55 m post-drug
J
Duration of Inhibition (s)
60 min

FIGURE S4. Effect of intra vlPAG microinjection of AM251 (0.25, 0.5 and 1 nmol) on the spontaneous and noxious-evoked activity of RVM ON and OFF cells in lean and *ob/ob* mice. **(A, B)** Representative rate histograms illustrate the pro-nociceptive effect exerted by the intermediate dose of AM251 on the ON cell activity in *ob/ob* mice starting 20 minutes after the injection, whereas the same dose of AM251 did not exert any effect in lean mice. Sixty minutes of recording are shown. **(C)** Representative immunoblots from CB_1/β-arrestin2 co-immunoprecipitation assays showing a basal levels of CB_1/β-arrestin2 complexes more expressed in *ob/ob* mice compared to wt. Note, the effect of OX-A on the elevation of CB_1/β-arrestin2 complexes is reversed by pretreatment with the OX1-R antagonist (SB334867,30mg/kg in wt mice and 60mg/kg in *ob/ob* mice; i.p., 30 min). ** $P < 0.005$ (P=0.003; $F_{(1,15)}$=42.26) by comparison of *ob/ob* mice in control condition *vs* wt+SB, *ob/ob*+SB, wt+SB+OX-A and *ob/ob*+SB+OX-A. ° $P < 0.005$; (P=0.002; $F_{(1,17)}$=40.78) by comparison of wt+OX-A *vs* wt in control condition and *vs* wt+SB. # $P < 0.05$ (P=0.03; $F_{(1,14)}$=12.18) by comparison of wt+OX-A *vs* wt+SB+OX-A). Each column represents the mean ± SEM of n= 3 mice. Statistical analysis was performed by two-way ANOVA test followed by Bonferroni *post-hoc* test. **(D-F)** Neuronal population data of the ON cell evoked activity showing that AM251 significantly reduced the onset (**D**), and increased the duration of excitation (**E**) and the evoked frequency (**F**) in both lean and *ob/ob* mice, but at different doses (1 and 0.5 nmol, respectively). The onset in lean mice was 158 ± 22.89 ms (P=0.00; $F_{(1,11)}$=162.02), 20 min after the AM251 microinjection, compared to the basal values (766 ± 39.45 ms), and in *ob/ob* mice was 558 ± 67.85 ms (P=0.00; $F_{(1,13)}$=49.45), 20 min after the AM251 microinjection, compared to the basal values (1380 ± 98.24 ms). The duration of excitation did not differ between lean and *ob/ob* mice in basal condition (3.36 ± 0.71 s and 3.3 ± 0.43 s, respectively) while it increased 20 min after AM251 microinjection both in lean (12.2 ± 0.86 s, P=0.00; $F_{(1,11)}$=64.05) and *ob/ob* (12.5 ± 0.8 s, P=0.00; $F_{(1,13)}$=94.2) mice. Also the evoked frequency increased both in lean (26.33 ± 1.2 Hz *vs* basal values 19.8 ± 1 Hz, P=0.001; $F_{(1,11)}$=17.79) and in *ob/ob* (21.2 ± 1.15 Hz *vs* basal values 9.78 ± 0.99 Hz, P=0.00; $F_{(1,13)}$=54.93). **(G, I)** Representative rate histograms illustrate the pro-nociceptive effect exerted by the intermediate dose of AM251 on the OFF cell activity in *ob/ob* mice, starting 15 minutes after the injection, whereas the same dose did not exert any effect in lean mice. Sixty minutes of recording are shown. **(H,J)** Neuronal population data of the OFF cell evoked activity show that AM251 significantly reduced the onset **(H)**, and increased the duration of inhibition **(J)** in both lean and *ob/ob* mice, but at different doses (1 and 0.5 nmol, respectively). The onset in lean mice was 180 ± 21.68 ms (P=0.00; $F_{(1,12)}$=56.62), 20 min after the AM251 microinjection, compared to the basal values (776 ± 87.9 ms), and in *ob/ob* mice was 474 ± 45.78 ms (P=0.00; $F_{(1,13)}$=92.76), 20 min after the AM251 microinjection, compared to the basal values (1296 ± 75.48 ms). The duration of inhibition increased in both lean

(19.60 ± 0.92 s *vs* basal values 11.60 ± 1.64 s, P=0.00; $F_{(1,12)}$=20.56) and *ob/ob* (20.2 ± 0.86 s *vs* basal values 4.4 ± 0.8 s, P=0.00; $F_{(1,11)}$=176.51) mice. Each column represents the mean ± SEM of n=6-8 mice per group and one neuron was recorded for each animal. ° $P < 0.05$ indicates significant difference of lean+AM251 1 nmol v*s* lean+AM251 0.5 nmol, $^{\#}P < 0.05$ indicates significant of *ob/ob*+AM251 0.5 nmol v*s* *ob/ob*+AM251 0.25 nmol. The solid and dashed lines represents the wt and *ob/ob* basal value, respectively. *P* values indicate statistically significant difference by two-way ANOVA followed by Bonferroni *post-hoc* test.

Figure S5

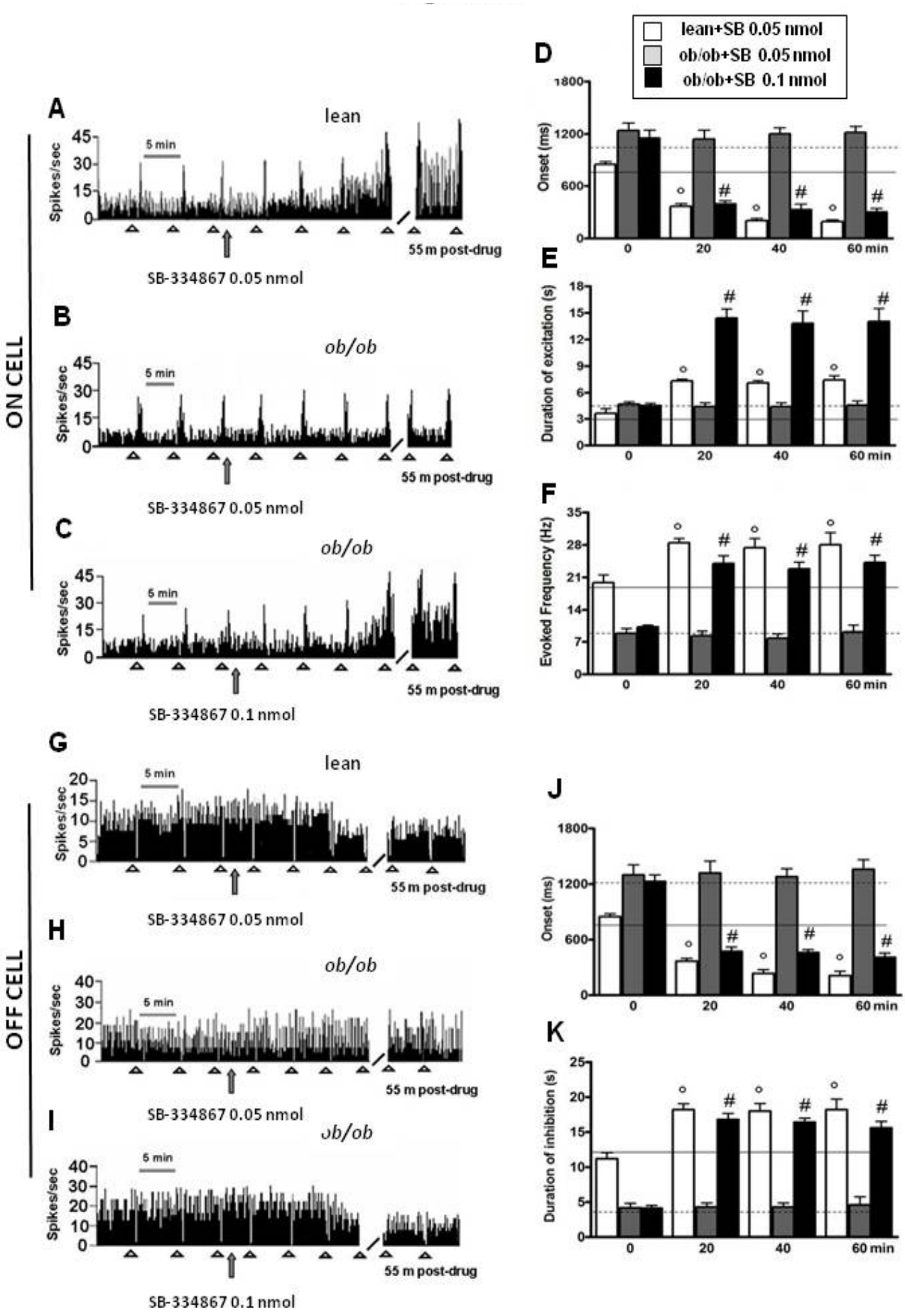
ON CELL
OFF CELL
A
lean
B
ob/ob
C
ob/ob
G
lean
H
ob/ob
I
ob/ob
Spikes/sec
5 min
55 m post-drug
SB-334867 0.05 nmol
SB-334867 0.1 nmol
D
lean+SB 0.05 nmol
ob/ob+SB 0.05 nmol
ob/ob+SB 0.1 nmol
Onset (ms)
E
Duration of excitation (s)
F
Evoked Frequency (Hz)
J
Onset (ms)
K
Duration of inhibition (s)
0
20
40
60 min

FIGURE S5. Effect of intra vlPAG microinjection of SB334867 (0.05 and 0.1 nmol) on the spontaneous and noxious-evoked activity of RVM ON and OFF cells in wt and *ob/ob* mice. **(A-C)** Representative rate histograms illustrate the pro-nociceptive effect exerted by the highest dose in *ob/ob* mice and by the lowest dose in wt mice of SB334867 on the ON cell spontaneous and evoked activity. The low dose of SB334867 did not change the ON cell activity in *ob/ob* mice. Sixty minutes of recording are shown. **(D-F)** Neuronal population data of the ON cell evoked activity showing that SB334867 significantly reduced the onset (**D**), and increased the duration of excitation (**E**) and the evoked frequency (**F**) in both wt and *ob/ob* mice, but at different doses (0.05 and 0.1 nmol, respectively). The onset in wt mice was 370 ± 22.25 ms, 20 min after the SB334867 microinjection, compared to the basal values (790 ± 26.27 ms), and in *ob/ob* mice was 394 ± 37 ms, 20 min after the SB334867 microinjection, compared to the basal values (1164 ± 84.24 ms). The duration of excitation did not differ between wt and *ob/ob* mice in basal condition (3.36 ± 0.71 s and 4.48 ± 0.3 s, respectively), while it increased 20 min after SB334867 microinjection in both wt (7.26 ± 0.26 s) and *ob/ob* (14.4 ± 1 s) mice. Also the evoked frequency increased in both wt (28.4 ± 0.92 Hz *vs* basal values 19.2 ± 1 Hz) and in *ob/ob* (24 ± 1.64 Hz *vs* basal values 8.0 ± 0.69 Hz). **(G-I)** Representative rate histograms illustrate the pro-nociceptive effect exerted by the highest dose in *ob/ob* mice and by the lowest dose in lean mice of SB334867 on the OFF cell spontaneous and evoked activity. The low dose of SB334867 did not change the OFF cell activity in *ob/ob* mice. Sixty minutes of recording are shown. **(J,K)** Neuronal population data of the OFF cell evoked activity show that SB334867 significantly reduced the onset **(J)**, and increased the duration of excitation **(K)** in both lean and *ob/ob* mice, but at different doses (0.05 and 0.1 nmol, respectively). The onset in lean mice was 368 ± 30.62 (P=0.00; $F_{(1,13)}$=85.79), 20 min after the SB334867 microinjection, compared to the basal values (844 ± 39.82 ms), and in *ob/ob* mice was 468 ± 39.6 ms (P=0.00; $F_{(1,11)}$=92.76), 20 min after the SB334867 microinjection, compared to the basal values (1234 ± 70 ms). The duration in lean mice was 18.20 ± 0.86 ms (P=0.00; $F_{(1,13)}$=44.87), 20 min after the SB334867 microinjection, compared to the basal values (11.60 ± 1.71 s), and in *ob/ob* mice was 16.8 ± 0.86 s (P=0.00; $F_{(1,11)}$=71.5), 20 min after the SB334867 microinjection, compared to the basal values (4.4 ± 0.8 s). Each point represents the mean ± SEM of n=6-8 mice per group and one neuron was recorded for each animal. The solid and dashed lines represents the lean and *ob/ob* mean controlvalue, respectively. ° $P < 0.05$ indicates significant difference of lean+SB 0.05nmol v*s* lean mice (0 min) per each individual time points, $^{\#}$ $P < 0.05$ indicates significant difference of *ob/ob*+SB 0.1 nmol v*s* *ob/ob*+SB 0.05 nmol. *P* value was considered statistically significant using two-way ANOVA followed by the Bonferroni post-hoc test.

Figure S6

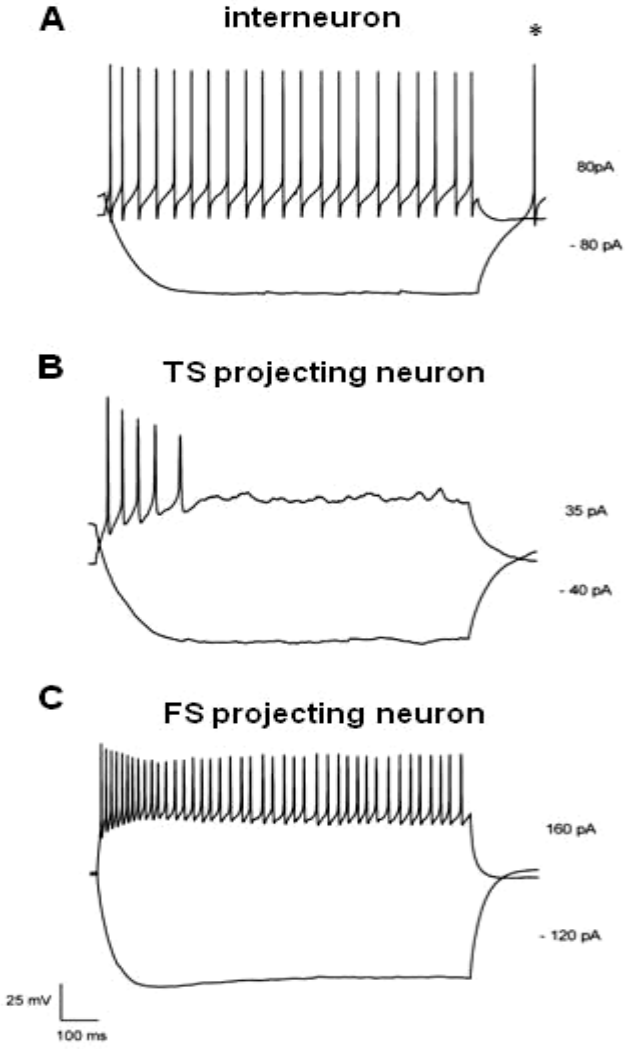

FIGURE S6. Electrophysiological Identification of vlPAG neurons projecting to RVM. Different intrinsic membrane properties of vlPAG neurons projecting to RVM and GABAergic interneurons allow their electrophysiological identification. (**A**) membrane properties of GABAergic interneurons, characterized by high frequent, non-adapting firing (frequency ≥ 20 Hz) evoked by a depolarizing current pulse and a low-threshold spike (LTS, *) during the repolarization phase. (**B, C**) membrane properties of the two types of vlPAG projecting neurons: transient spiking (TS; spike frequency < 20 Hz showing strong adaptation; **B**), and fast spiking (FS; frequency ≥ 20 Hz showing weaker adaptation; **C**). None of them express LTS as a reaction to a hyperpolarizing current pulse. Neurons were kept at -60 mV for the testing. The amount of applied current is indicated for each trace. Our recordings confirm previous description (Park et al., PNAS 2010) and extend to projecting neurons and interneurons of *ob/ob* mice.